2016 IEEE International Conference on Robotics and Automation (ICRA)
Stockholm, Sweden, May 16-21, 2016

KONTUR-2: Force-feedback Teleoperation from the International Space Station

Jordi Artigas, Ribin Balachandran, Cornelia Riecke, Martin Stelzer, Bernhard Weber, Jee-Hwan Ryu*, Alin Albu-Schaeffer

***Abstract*— This paper presents a new robot controller for space telerobotics missions specially designed to meet the requirements of KONTUR-2, a German & Russian telerobotics mission that addressed scientific and technological questions for future planetary explorations. In KONTUR-2, Earth and ISS have been used as a test-bed to evaluate and demonstrate a new technology for real-time telemanipulation from space. During the August 2015' experiments campaign, a cosmonaut teleoperated a robot manipulator located in Germany, using a force-feedback joystick from the Russian segment of the International Space Station (ISS). The focus of the paper is on the design and performance of the bilateral controller between ISS joystick and Earth robot. The controller is based on a 4-Channels architecture in which stability is guaranteed through passivity and the Time Delay Power Network (TDPN) concept. We show how the proposed approach successfully fulfills mission requirements, specially those related to system operation through space links and internet channels, involving time delays and data losses of different nature.**

I. Introduction

Telerobotics is one of the most succesful and versatile space technologies. In the last years there have been impressive space missions that involved the use of robots, showing their effectiveness in fields as diverse as Mars exploration, on-orbit servicing or meteorite sample and return. A common attribute of these robots is that they are controlled from Earth to perform some sort of manipulation of the environment along with some degree of autonomy. However, robotics hasn't yet shown its potential in missions that require high dexterity levels: The ISS is still fully maintained by astronauts; four manned servicing missions on the Hubble Space Telescope raised the original costs of $2.5B to $10B as of 2010 [1]. Robots are undeniably safer and more cost effective compared to on-site astronautic operations, though arguably, much more limited in terms of cognitive and manipulation abilities.

Real-time teleoperation is in these scenarios an appealing technology as it combines robotic capabilities with human intelligence and manipulation skills. Furthermore, it is a technology that has been thoroughly investigated for many years and finds itself in a rather mature stage.

The KONTUR-2 mission aims at achieving the next milestone in planetary exploration missions to allow astronauts to work with robots on the ground from an orbital station. To do that, KONTUR-2 will provide answers to the following scientific and technological questions:

- What are the communication requirements to teleoperate a robot manipulator in real time in space missions?
- What is the design of the controller that is capable of coping with latencies, data losses and other channel related characteristics while providing reliable force-feedback?
- What is the loss in human proprioception when controlling an Earth robot from the ISS, including the effects of time delay and microgravity effects?

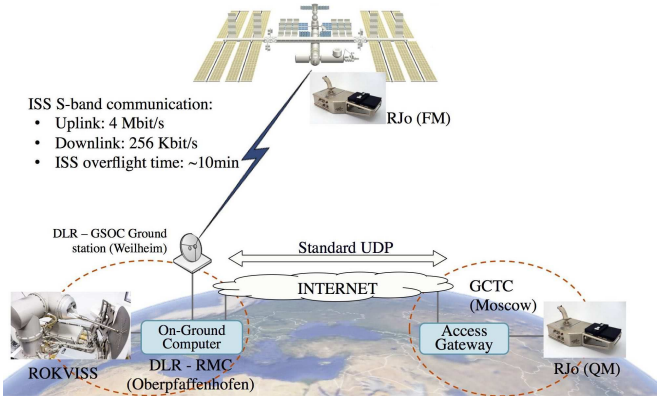

Fig. 1: KONTUR-2 scenarios

To answer these questions, a space qualified 2 degrees of freedom (DoF) force-feedback joystick was developed at the DLR and sent on July 24th to the Russian segment of the ISS. Mr. Oleg Kononenko, cosmonaut from Roscomos, performed a set of experiments that consisted of controlling ROKVISS, a 2 DoF robot manipulator located at the DLR (Oberpfaffenhofen, Germany) using the force-feedback joystick (see Fig. 1). The focus of the paper is on the first two questions. We first establish general control requirements for space telerobotics, based on results from a DLR trajectory that begins in 1993 with ROTEX, the first space robotics experiment [2], and goes on with 2015's KONTUR-2. The second block of the article presents a new bilateral control architecture that fulfills these requirements related to stability and performance. A major challenge in this context arises due to the communication delay and data losses of command signals from the human operator to the robot and the force signals back to the operator.

A joint treatment of these two areas, communication and control, is encouraged due to their strong interaction and

Authors are with the Institute of Robotics and Mechatronics in the German Aerospace Center (DLR), 82234 Wessling, Germany, email: jordi.artigas@dlr.de.

*Jee-Hwan Ryu is with the Korean Institute of Technology and Education (KOREATECH), Cheonan, South Korea

dependencies: On one hand, the control engineer needs to understand the properties of the communication channel such as to design the bilateral controller; on the other hand, the communication expert should take into account real-time requirements imposed by the bilateral controller. This control-communication interplay presents interesting trade-offs between the two areas with interesting repercussions; e.g. if the controller is capable of working in low bandwidths / high jitters settings it can potentially loosen requirements for the communication infrastructure.

II. Other existing similar methods

Stability and transparency in bilateral teleoperation have been in research since decades. Transparency as a trade-off for system stability has been discussed in [3] and [4]. The effects of internal time delay, sampling and quantization and the physical properties like inertia and damping on the stability of a haptic device have been studied in [5]. Passivity as a tool for stability to cope with communication delay was studied in [6] and [7], where the teleoperation system is modelled based on transmission lines equations (aka. scattering parameters and wave variables). [8], [9] have extended these ideas using port-Hamiltonians, an energy based modelling tool that allows more complex control structures.

On the other hand, the Time Domain Passivity Approach (TDPA) analyses system passivity in real-time and bases its control on the observability of the system energy and a variable damping injection that acts during active phases of operation [10]. It was extended to time delayed teleoperation based on the Time Delay Power Networks (TDPN) representation in [11] and [12]. The authors of [13] presented a 4-channels architecture that is based on two TDPNs carrying force signals. However, sending explicit position signals, as will be shown in Sec. V, is beneficial as it significantly improves position tracking performance [14].

III. ISS and Training communication requirements

Table I shows communication parameters registered during the main DLR telerobotics missions.

Experiment	Type	T. Delay	P. Loss	Bandwidth
Rokviss	ISS Link	20-30 ms	0.1%	245Kbps/4Mbps
Artemis	GEO-Sat	620 ms	5.8%	4Mbps
Astra	GEO-Sat	540 ms	2.6%	4Mbps
K2 Training	Internet UDP	65 ms	7%	10Mbps

TABLE I: Main DLR space telerobotics missions communication parameters (see Appendix for the missions descriptions)

As it can be seen, time delay varies substantially depending on the particular communication infrastructure. Geostationary satellite communications (ASTRA, ARTEMIS) average higher than 0.5 seconds [15], [16]. The direct link used in ROKVISS on the other hand presents lesser delay.

In KONTUR-2, two scenarios had to be considered in the design of the bilateral controller: ISS and training. The first is the nominal mission case, where the cosmonaut controls the robot from the ISS through a S-band link. The second, is a geographically distributed scenario for cosmonaut training purposes (see Fig. 1). Since the exact same system needs to operate in both, the requirements for the bilateral controller are clearly strengthened as both links are characterized by different communication parameters.

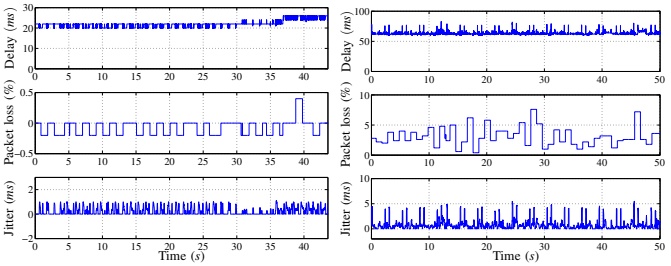

(a) Comm. Pars. ISS link (b) Comm. Pars. GCTC internet link

Fig. 2: Space and Internet links parameters

The cosmonaut training took place at the Gagarin Research and Test Cosmonaut Training Center (GCTC), located in Moscow. During the training, the cosmonaut practiced with a joystick qualification model (QM) with identical characteristics of the ISS flight model (FM), and controlled the robot located at the DLR, in Germany, through the internet.

Fig. 2(a) and Fig. 2(b) show the performance of ISS and internet UDP links. The nature of these two links is quite different in terms of time delay, data losses and jitter. The time delay for the ISS communication varied from 20 to 30 *ms* (corresponding to azimuth and horizon points) with mean negligible data losses. The internet training setup introduced a mean delay of 65 *ms* and highly oscillating package loss ratio, from 5% to 7% (due to the UDP protocol). Though more limited in bandwidth, the ISS link is higher in performance. However, shadowing can occur resulting in signal attenuation and in turn higher package loss ratios or even communication blackouts. On the other hand, the internet link measurements confirm a typical UDP behaviour.

The bilateral controller presented in this paper is aimed at generality: the main control requirements (related to the communication parameters) is to guarantee stability and to maximize performance in any of the above mentioned conditions, including those of Table I.

IV. Energy, time delay and passivity

One of the major challenges in designing the bilateral controller is the treatment of package loss and jitter factors. Most approaches are capable of handling constant small and large time delays. Although there have been remarkable steps for making these approaches robust against jitter and package losses (see references in Sec. II), the rationale that sustains them assumes a constant or even previously known time delay. As already mentioned, the control method presented in this paper is based on the Time Domain Passivity Control approach. One of the main benefits of this approach is that jitter and data losses are naturally handled by the approach since both factors result in variations of the system energy.

The well known passivity theory provides a tool to determine a relationship between time delay and energy that is useful for analyzing the stability of feedback systems. In particular,

$$\int_0^\infty u(\tau)^* v(\tau) dt + C \geq 0, \quad (1)$$

establishes that if the time integral of the dual product between two power correlated signals, u and v, is greater than or equal to zero, the system is passive, meaning that it cannot generate more energy than the stored amount, C. It has been proved that if there is a phase lag (or delay in time units) between one of the above correlated signals w.r.t. the other, the passivity rule is violated, resulting in a non-passive system and in turn potentially unstable. The use of passivity in control has been a matter of controversy. Arguably, forcing a system to be passive to ensure stability is a conservative criterion since passivity is not a necessary but rather a sufficient condition for stability. Nevertheless, passivity presents some unique features that are beneficial in real-time telerobotics:

1) Less dependency on plant models: Rather than looking at the particular internals of the controlled plant such as to obtain a transfer function, energy can be used as a control variable by checking the input/output signals of the plant.
2) It is *delay friendlier* (than other well established methods that are based on the analysis of transfer functions) since time delay naturally modifies the passivity property of the system and this can be easily observed.
3) Non-continuous factors as jitter and data losses can be well embedded within the same control framework since they all naturally have impact on passivity as well.

Clearly, these are important values in order to satisfy the above established mission requirements.

Briefly, the TDPA has two main elements: the Passivity Observer (PO), which monitors the energy flow of a network in time domain; and the Passivity Controller (PC), which acts as a variable damper to dissipate the energy introduced by the network. See [12] for a review on the TDPA approach. In order to expose the underlying ideas of the bilateral controller presented in the next section, the following tools and elements will be used:

- Passivity Controller (PC) and Passivity Observer (PO) as fundamental stability tool.
- Time Delay Power Network (TDPN), as a two-port network that models an energy consistent communication channel, with well defined effort and flow signals.
- A passivated TDPN, that is, a TDPN with a PC system (i.e. one PC at one or both sides[1] of the TDPN is required to make it passive).

Then, the following steps will lead to the control scheme presented in this paper:

[1]Depending on the specific system [11]

1) Design of the control scheme in an ideal setting, that is, neglecting time delays, jitter and package loss, using the conventional flow diagrams.
2) Representation of the control scheme in the electrical domain, using one-port and two-port networks.
3) Adding time delay source into the above scheme (through dependent flow and effort sources).
4) Unfoldment of the system TDPNs.
5) Passivate each TDPN through PCs, creating a TDPN-PC systems.

The above elements and steps are in the following section described.

V. Controller Design

In general, the design of a bilateral controller can be split into two parts: The architecture, which defines the bilateral data exchange and control between master and slave (e.g. position-force) and the stability mechanism, which ensures stable operation under some desired conditions.

4-channels architectures, i.e. exchanging force and position signals between both master and slave, reach highest performance degrees since they can theoretically reach ideal transparency in the non-delayed case [3], [17]. They are also higher in complexity and require higher communication bandwidths than 2-channels architectures (e.g. position-force). In KONTUR-2, the S-Band space link has a capacity of 256 Kbps for the uplink and 4 Mbps for the downlink (see Fig. 1). It can be easily proved that this bandwidth is sufficient for a 500Hz transmission rate, a 2 DoF system with a 4-channels architecture and a coding of 2 bytes per signal.

Thus, the chosen architecture is defined by two forward channels carrying master position and force signals, and two feedback channels, carrying slave computed and measured force signals (see Fig. 3). The main reason for choosing this architecture instead of the symmetric 4-channels, with position and force in both directions, is to reduce the spring-like characteristic caused by the delayed position closed loop, which can be disturbing, specially for substantial or varying delays. Note that in this new configuration, position tracking can still be achieved since the slave remains linked in position to the master.

On the other hand, the duality in the force feedback signal presents interesting properties: The low-pass characteristic of the computed force channel, given by the spring-damper of the slave Proportional-Integral (PI) controller, allows to set higher gain values for the measured force channel (which is typically more prone to instabilities). This second channel, in turn, also contains the high frequency information of the telemanipulation (only limited by the force sensor capabilities and the slave control cycles). A thorough analysis of the interplay between these two channels and how they affect each other in terms of stability and performance is out of the scope of this article and will be presented in future works.

On the forward path, the combination of a position and a (measured) force channel presents two main benefits: Convergence to zero of master-slave position error and partial

masking of the slave dynamics thanks to the feedforward force term.

The stability mechanism is entirely underpinned on the TDPN representation. Roughly, TDPNs provide an augmented network representation of the system that allows to explain the energy exchange within the system that contains one or more time delays (see Appendix for further details).

The design steps defined in the previos section are explained in the following subsections.

A. Design of the control scheme: Block diagram

Rather than focusing on how to tune the channels (thoroughly studied in the mentioned references), a properly tuned system is hereby assumed, that is, the controller gains have been adjusted so as to ensure stability in the non-delayed case and to satisfy some performance goals. The design is

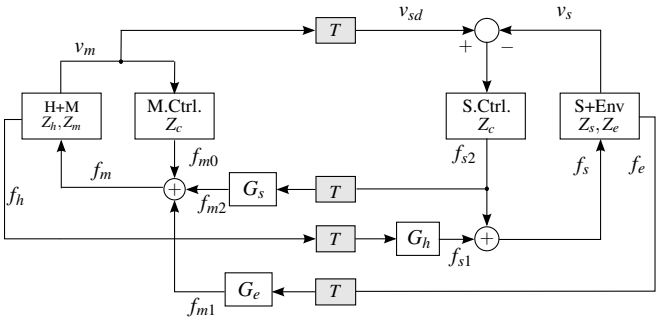

Fig. 3: Block diagram of a 4-Channels architecture

shown in Fig. 3. The causality on both, master and slave systems, is impedance, that is, the commanded signal is a force and the output is position (or velocity, analogously). Postion tracking is established through the PI controller with transfer function $Z_c(s) = \frac{K_{ds}s+K_{ps}}{s}$. The force commands at both sides are derived by:

$$\begin{aligned} f_s(t) &= G_h f_h(t-T) + K_{ds}(v_m(t-T) - v_s(t)) \\ &\quad + K_{ps}(x_m(t-T) - x_s(t)), \\ f_m(t) &= G_s f_{s2}(t-T) + G_e f_e(t-T) + K_{dm} v_m(t), \quad (2) \end{aligned}$$

where f_h, f_{s2}, f_e are human measured force, computed and measured forces at the slave side respectively; v_m, v_s are master and slave velocity signals respectively. Furthermore, the controller at the slave side is a Proportional-Integral with constants K_{ps} and K_{ds} and the master has a local damper with value K_{dm}. G_h, G_s and G_e are scaling factors to match both system dynamics. Forward and backward delays, T, are assumed to be equal for the sake of simplicity. The transfer function in the Laplace domain of the block containing the human and the master device, $H+M$, can be modeled as:

$$\begin{aligned} (f_h(s) - f_m(s)) \frac{1}{m_m s^2 + b_m s} &= x_m(s), \\ f_h(s) &= v_m(s) Z_h(s), \quad (3) \end{aligned}$$

where m_m and b_m are master mass and damping coefficients, and Z_h is the human impedance. Equations at the slave side can be obtained in a similar way.

B. Representation of the (delayed) control scheme in the electrical domain

In order to extract the TDPNs of the system, the analogous electrical representation is needed. Applying the classical force-voltage / velocity-current analogy, the system in Fig. 3 can be represented in the electrical domain as shown in Fig. 4. As it can be seen, the communication channels are represented through dependent force and velocity sources (see [11]), leading to four delayed dependent sources: Three for the force signals transmission, and one for the velocity signal transmission. Note the series interconnection at master and slave sides to produce the force commands [2], $f_m = f_{m1} + f_{m2}$ and $f_s = f_{s1} + f_{s2}$. Furthermore, it can be easily seen that the system equations of the block diagram representation (2) hold in the new scheme.

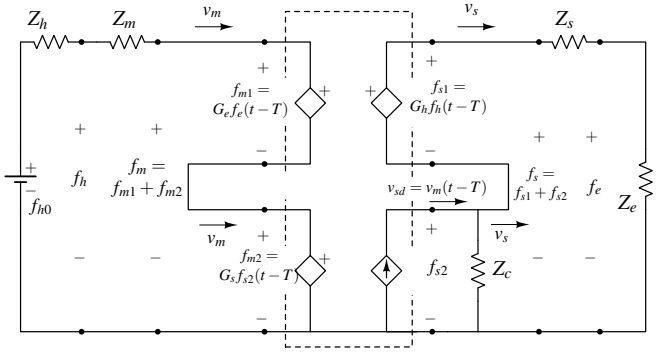

Fig. 4: Electrical scheme of a 4 Channels architecture

C. Unfoldment of the system TDPNs

The unfoldment of the TDPNs is carried out by looking at the dependent velocity and force sources. The TDPN allows to bring the source to its non-delayed location by providing a medium through which its signal can propagate.

Note that the same dependent source defines the port variables of the TDPN. Then, for each time dependent source a TDPN can be unfolded. See Fig. 5: The result is a scheme with four TDPNs, one for each channel.

1) TDPN A: Conveys measured force (source C_a) from slave to master
2) TDPN B: Conveys computed force (source C_b) from slave to master
3) TDPN C: Conveys measured force (source C_c)from master to slave
4) TDPN D: Conveys velocity (source C_d) from master to slave

Note that the TDPNs preserve the original correlated variables pairs (e.g. f_{m1} and v_m at TDPN A's left port corresponds to the upper left force dependent source port in Fig. 4) and so the system equations hold). Morevover, it can be noted a zero delay value, $T = 0$, leads to the original scheme in Fig. 4 as the TDPNs naturally vanish.

[2] A local damper at the master side of $K_{dm} = 0$ is considered in this representation to simplify the analysis

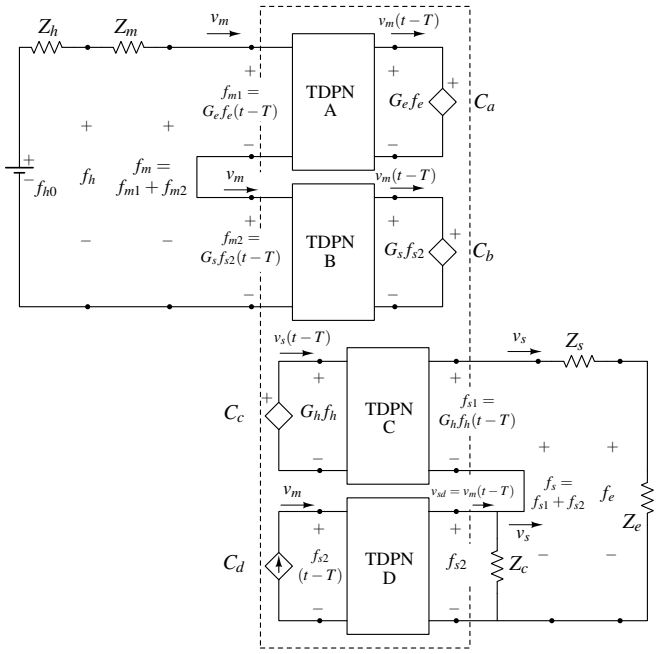

Fig. 5: 4 Channels architecture augmented with a pair of TDPNs

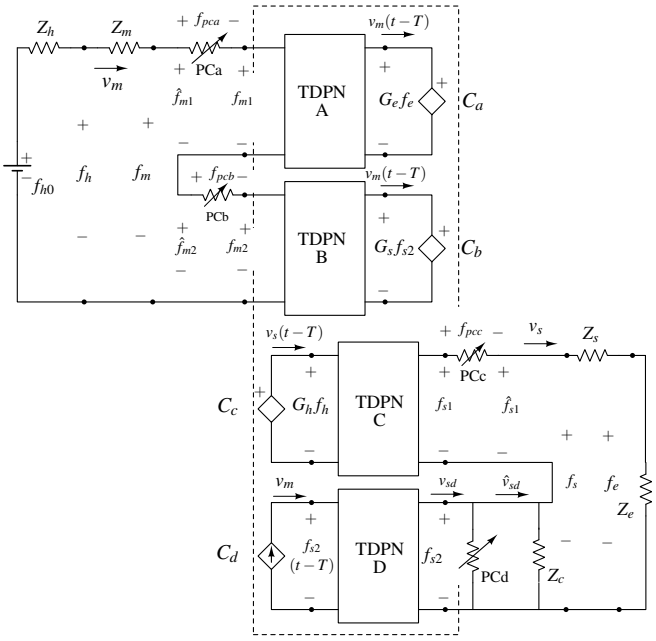

Fig. 6: Four channel architecture with the Passivity Controllers

The electrical scheme tells us the conjugate pairs at each TDPN network port:

$$\text{TDPN A}: \begin{cases} \langle \; G_e f_e(t-T) \;,\; v_m(t) \; \rangle & \text{at the master} \\ \langle \; G_e f_e(t) \;,\; v_m(t-T) \rangle & \text{at the slave} \end{cases}$$

$$\text{TDPN B}: \begin{cases} \langle \; G_s f_{s2}(t-T) \;,\; v_m(t) \; \rangle & \text{at the master} \\ \langle \; G_s f_{s2}(t) \;,\; v_m(t-T) \rangle & \text{at the slave} \end{cases}$$

$$\text{TDPN C}: \begin{cases} \langle \; G_h f_h(t) \;,\; v_s(t-T) \; \rangle & \text{at the master} \\ \langle \; G_h f_h(t-T) \;,\; v_s(t) \; \rangle & \text{at the slave} \end{cases}$$

$$\text{TDPN D}: \begin{cases} \langle \; f_{s2}(t-T) \;,\; v_m(t) \; \rangle & \text{at the master} \\ \langle \; f_{s2}(t) \;,\; v_m(t-T) \; \rangle & \text{at the slave} \end{cases}$$

D. Final scheme: Four channel , TDPN based passive system

The augmented, TDPN based representation reveals the energy sources caused by the time delay (along with jitter and package loss), i.e., TDPN A to D. These two-port networks are indeed non-passive and will most likely make the system unstable, even for small amounts of delay (e.g. 5ms[3]). Passivation of two-port networks can be easily achieved by placing one Passivity Controller at the TDPN port, as shown in [18], [12].

The scheme with the passivated TDPNs is shown in Fig. 6. As it can be seen, a PC is connected to each TDPN: PCa, PCb, PCc and PCd. In the following, we show the development of PCb, corresponding to TDPN B. The same rationale is then applied for the remaining TDPNs.

[3]Depending on the particular PI controller parameters, local dampers and gain factors

TDPN B: The energy of the TDPN B W_{Mb}, observed by the PO, is given by:

$$W_{Mb}(n) \;=\; E_{in}^{Sb}(n-D) - E_{out}^{Mb}(n) + E_{PC}^{Mb}(n) \qquad (4)$$

where D represents a discrete communication time delay. Furthermore,

- $E_{in}^{Sb}(n-D)$ is the delayed energy entering (subscript *in*) the TDPN from the slave side (superscript *Sb*), observed at the master side
- $E_{out}^{Mb}(n)$ is the energy exiting (subscript *out*) the TDPN at the master side (superscript *Mb*) and
- $E_{PC}^{Mb}(n)$ is the energy dissipated by the passivity controller of TDPN B

E_{in}^{Sb} and E_{out}^{Ma} are computed by adding the power contribution at the corresponding ports, P_{in}^{Sb} and P_{out}^{Mb} and taking into account the direction of the energy flow and T_s being the sampling time:

$$E_{in}^{Sb}(n) \;=\; E_{in}^{Sb}(n-1) + T_s P_{in}^{Sb}(n) \qquad (5)$$

$$E_{out}^{Mb}(n) \;=\; E_{out}^{Mb}(n-1) + T_s P_{out}^{Mb}(n) \qquad (6)$$

$$P_{in}^{Sb}(n) = \begin{cases} f'_{s2}(n)(-v_m(n-D)) & \text{if } f'_{s2}(n)(-v_m(n-D)) > 0 \\ 0 & \text{else} \end{cases}$$

$$P_{out}^{Mb}(n) = \begin{cases} f'_{s2}(n-D)(-v_m(n)) & \text{if } f'_{s2}(n-D)v_m(n) < 0 \\ 0 & \text{else,} \end{cases}$$

where $f'_{s2}(n) = G_s f_{s2}(n)$ is the scaled feedback force. Note that all energy signals are positive defined.

The main goal of the passivity controller is to ensure that the observed energy will be equal or greater than zero, that is, $W_{Mb}(n) \geq 0 \quad \forall n \geq 0$. The controller is thus defined as:

$$f_{m2}(n) = G_s f_{s2}(n-D) - v_m(n)\alpha_b(n), \qquad (7)$$

where the dissipation factor, α_b, is given by:

$$\alpha_b(n) = \begin{cases} 0 & \text{if } W_{Mb}(n) > 0 \\ \dfrac{-W_{Mb}(n)}{T_s v_m^2(n)} & \text{else} \end{cases}$$

Applying (7) ensures that the energy flowing out of the TDPN through the left port, E_{out}^{Mb}, is modified such that it is bounded by the delayed entering energy at the right port, $E_{in}^{Sb}(n-D)$. The modified energy signal is then given by

$$\hat{E}_{out}^{Mb}(n) = E_{out}^{Mb}(n) - E_{PC}^{Mb}(n). \tag{8}$$

It can be easily proved that this modified energy satisfies the passivity condition, $W_{Mb}(n) \geq 0$, i.e., the network created by the TDPN plus the PC is a passive one. Furthermore, the energy dissipated by the PC is given by:

$$E_{PC}^{Mb}(n) = T_s \sum_{k=1}^{n-1} v_m^2(k)\alpha_b(k), \tag{9}$$

On the other hand, TDPN D is of velocity type (see [18]). As such, it has a parallel PC located on the slave side port to dissipate energy by modifying the velocity command $v_{sd} = v_m(t-T)$ to $\hat{v}_{sd}(t)$, as shown in Fig. 6. Over-dissipation of this controller can occur and potentially lead to position drift. This effect is however compensated using the enhanced Passivity Controller proposed in [14].

VI. Results

As explained in Sec. I, the experiments were conducted in two different setups: The real mission scenario with the direct Earth-ISS S-Band link, and the cosmonaut training scenario, through standard UDP internet link. In both cases, the proportional control parameter is chosen to be $K_{ps} = 80Nm/rad$ and the local damper of the master is $K_{dm} = 0.07Nms/rad$. The scaling factors for TDPNs A, B and C have values of $G_e = 0.006$, $G_s = 0.003$ and $G_h = 40$ respectively, to match the dynamics of both systems. Joystick and ROKVISS are dynamically very different, with maximum torques of 0.2Nm and 40Nm respectively.

The performance of the controller for both scenarios are shown in the following plots. Fig. 7 and Fig. 8 show the results of an experiment session conducted during August 25th 2015 with cosmonaut Mr. Kononenko. These plots show the position tracking and the force feedback performance during rigid contact situations and for free environment respectively. The rigid contact and free environment motion during the cosmonaut training that took place at GCTC in Moscow (joystick) and the DLR (ROKVISS robot), are shown in Fig. 9 and Fig. 10.

Fig. 11 show the observed energies of TDPN C and D. As it can be seen, outgoing energies, E_x^{out}, are greater than incoming energies, E_x^{in}, indicating an active behaviour of the TDPNs. The modified energy values, $\hat{E}_x^{out}$ are however bounded by the incoming energies, showing the passivation of the TDPNs (see analogous energy definitions for TDPN B in Sec. V-D)

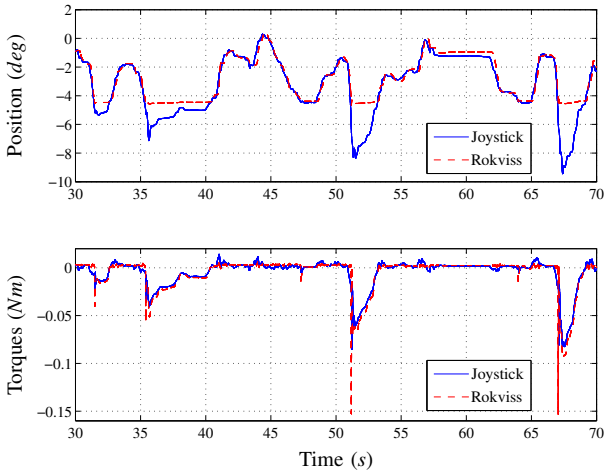

Fig. 7: Position and torques with rigid contacts during the mission

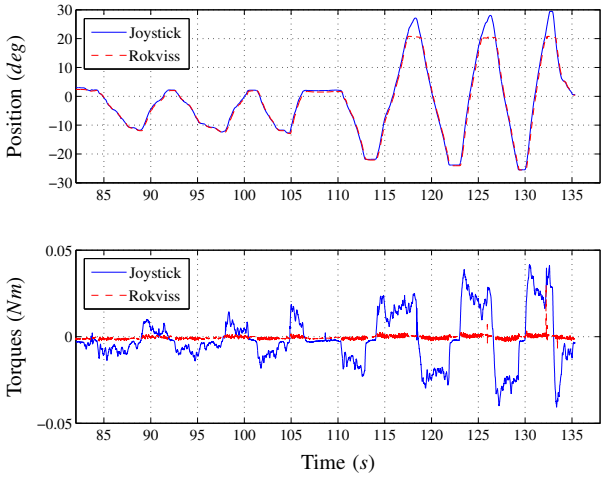

Fig. 8: Position and torques for free environment motion during the mission

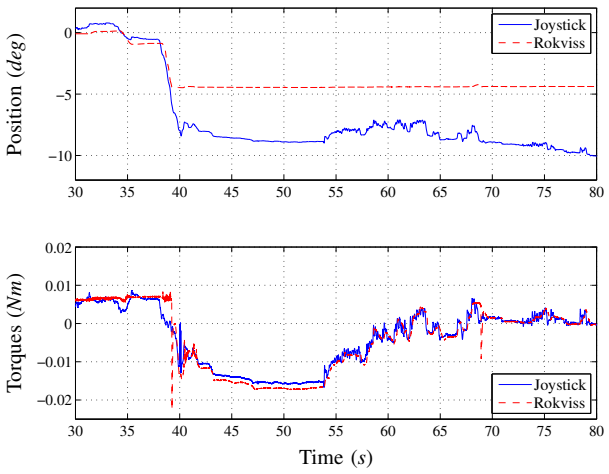

Fig. 9: Position and torques with rigid contacts during training

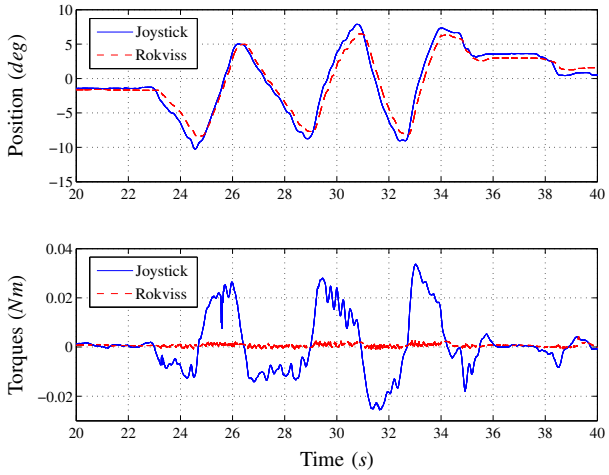

Fig. 10: Position and torques for free environment motion during training

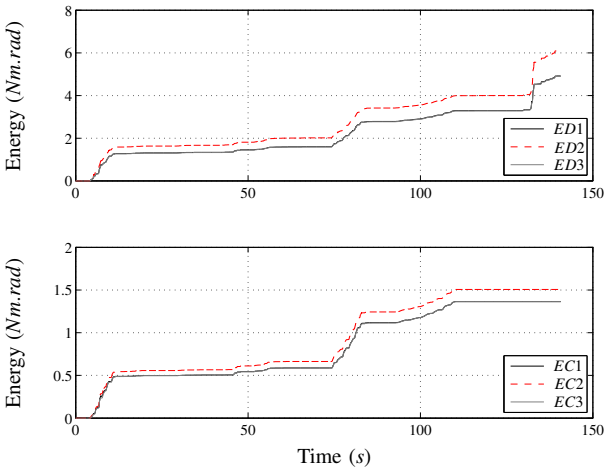

Fig. 11: Energies of TDPN C and D: $EC1 = E_{in}^{Mc}(t-T)$; $EC2 = E_{out}^{Sc}(t)$; $EC3 = \hat{E}_{out}^{Sc}(t)$; $ED1 = E_{in}^{Md}(t-T)$; $ED2 = E_{out}^{Sd}(t)$; $ED3 = \hat{E}_{out}^{Sd}(t)$

VII. Conclusions

The main contribution of this paper is the development of a 4-channels architecture based on the TDPN representation to achieve a controller design that is robust against a wide range of communication parameters, including delays, data losses and jitters. One of the most intersting features of this approach is that a system tuned for a setting close to ideal can operate in the conditions described in Sec. III. This is possible because the main cause for instability has been isolated from the rest of the system (TDPNs) and addressed in an adaptive fashion (Passivity Controller). The main novelty is the finding of the energy flows caused by the communication of 4-channels architectures (TDPNs A to D). Once these flows are uncovered, passivity control ensures that these networks remain passive and therefore, the system stable. Future work will deal with performance limitations and comparison to other control architectures. The next milestone in the KONTUR-2 mission will deal with the teleoperation of a humanoid robot located at the DLR from the ISS, involving higher DoFs and complex telemanipulation tasks.

VIII. Appendix

A. Definitions

1) DLR space telerobotics experiments:

- ROKVISS (2005) The first teleoperated robot in space with force-feedback from Earth. The same link point-to-point as for the KONTUR-2 space mission was used.
- SFB453-ARTEMIS experiment (2008): An experiment for testing the feasibility of geostationary communications using the ARTEMIS satellite for force-feedback teleoperation [15].
- FORROST-ASTRA experiment (2014): An experiment for testing the feasibility of geostationary communications using the ASTRA satellite for on-orbit servicing [16].

2) Time Delay Power Networks: By definition, a TDPN is a two-port (power consistent) network that conveys the energy of one particular signal from one point of the system to another, as for instance a force or a velocity signal. In a digital world, a force signal that is sent from one computer to another incurs a time delay. This is common even in digital systems, however such an event does not have a physical correspondence since e.g a force on its own *cannot propagate*. In a way, the TDPN provides an energy interpretation to that propagating force signal. By using this representation, energy flows that are not visible in common modelling tools (e.g. flow diagrams) become apparent. Once the flows are identified, their carriers, i.e. the TDPNs, are found to be the principal cause of instability. Passivity control can be then applied on each TDPNs in order to guarantee the stability of the system in the presence of delays, jitters and data losses [19].

Acknowledgments

The authors would like to thank the project partners ROSKOSMOS, RSC "Energia", RTC, the cosmonauts Oleg Kononenko and Sergej Volkov. Thanks also to the rest of the KONTUR-2 team and DLR colleagues who made possible and supported the development of the mission: Simon Schaetzle, Alexander Beyer, Michael Steinmetz, Bernhard Brunner, Peter Birkenkampf, Joerg Vogel, Klaus Jöhl, Stefan Kühne, Klaus Kunze, Henning Mende and Benedikt Pleintinger.

References

[1] J. William F. Ballhaus, *James Webb Space Telescope (JWST) Independent Comprehensive Review Panel (ICRP) Final Report*, ser. NASA contractor report. National Aeronautics and Space Administration, Scientific and Technical Information Branch, 2010, no. v. 3.

[2] G. Hirzinger, "Rotex the first space robot technology experiment," in *Experimental Robotics III*, ser. Lecture Notes in Control and Information Sciences, T. Yoshikawa and F. Miyazaki, Eds. Springer Berlin Heidelberg, 1994, vol. 200, pp. 579–598. [Online]. Available: http://dx.doi.org/10.1007/BFb0027622

[3] D. A. Lawrence, "Stability and transparency in bilateral teleoperation," *IEEE Transactions on Robotics and Automation*, vol. 9, no. 5, pp. 624–637, 1993.

[4] Y. Yokokohji and T. Yoshikawa, "Bilateral Control of Master-Slave Manipulators for Ideal kinesthetic Coupling – Formulation and Experiment," *IEEE Transactions on Robotics and Automation*, vol. 10, no. 5, pp. 605–620, October 1994.
[5] T. Hulin, A. Albu-Schaffer, and G. Hirzinger, "Passivity and stability boundaries for haptic systems with time delay," *Control Systems Technology, IEEE Transactions on*, vol. 22, no. 4, pp. 1297–1309, 2014.
[6] R. J. Anderson and M. W. Spong, "Bilateral Control of Teleoperators with Time Delay," *IEEE Transactions on Automatic Control*, vol. 34, no. 5, pp. 494–501, May 1989.
[7] G. Niemeyer, "Using wave variables in time delayed force reflecting teleoperation," Ph.D. dissertation, Massachussetts Institute of Technology, Sep. 1996.
[8] C. Secchi, C. Fantuzzi, and S. Stramigioli, "Transparency in port-hamiltonian based telemanipulation," *Control of Interactive Robotic Interfaces: A Port-Hamiltonian Approach*, pp. 165–199, 2007.
[9] C. Secchi, S. Stramigioli, and C. Fantuzzi, *Control of interactive robotic interfaces A port-Hamiltonian approach*, ser. Springer Tracks in advanced robotics. New York: Springer Verlag, 2007, vol. 29.
[10] J. Ryu, D. Kwon, and B. Hannaford, "Stable Teleoperation with Time Domain Passivity Control," in *IEEE Intl. Conference on Robotics and Automation, ICRA*, Washington, DC, USA, May 2002, pp. 3260–65.
[11] J. Artigas, J. Ryu, C. Preusche, and G. Hirzinger, "Network representation and passivity of delayed teleoperation systems." in *IROS*. IEEE, 2011, pp. 177–183.
[12] J. Ryu, J. Artigas, and C. Preusche, "A passive bilateral control scheme for a teleoperator with time-varying communication delay," *Elsevier Journal of Mechatronics*, vol. 20, pp. 812–823, October 2010.
[13] J. Rebelo and A. Schiele, "Time domain passivity controller for 4-channel time-delay bilateral teleoperation," *Haptics, IEEE Transactions on*, vol. 8, no. 1, pp. 79–89, 2015.
[14] J. Artigas, J. Ryu, and C. Preusche, "Position drift compensation in time domain passivity based teleoperation," in *IEEE International Conference on Robotics and Intelligent Systems*, Taipei, Taiwan, April 2010.
[15] E. Stoll, U. Walter, J. Artigas, C. Preusche, P. Kremer, G. Hirzinger, J. Letschnik, and H. Pongrac, "Ground verification of the feasibility of telepresent on-orbit servicing," *J. Field Robot.*, vol. 26, no. 3, pp. 287–307, Mar. 2009. [Online]. Available: http://dx.doi.org/10.1002/rob.v26:3
[16] R. Lampariello, N. Oumer, J. Artigas, W. Rackl, G. Panin, R. Purschke, J. Harder, U. Walter, J. Frickel, I. Masic, K. Ravandoor, J. Scharnagl, K. Schilling, K. Landzettel, and G. Hirzinger, "Forrost: Advances in on-orbit robotic technologies," in *Aerospace Conference, 2015 IEEE*, March 2015, pp. 1–20.
[17] K. Hashtrudi-Zaad and S. Salcudean, "On the Use of Local Force Feedback for Transparent Teleoperation," in *Proceedings of the 1999 IEEE International Conference on Robotics and Automation*, Detroit, Michigan, USA, May 1999.
[18] J. Artigas, J.-H. Ryu, and C. Preusche, "Time domain passivity control for position - position teleoperation architectures," *In MIT Journals Presence: Teleoopearators and Virtual Environments*, 2010.
[19] J. Artigas, "Time Domain Passivity Control for Delayed Teleoperation," Ph.D. dissertation, Universidad Politecnica Madrid - UPM, 2014.